50-GHz-bandwidth Electro-absorption Modulator with Membrane InGaAsP Lateral p-i-n Diode on Si Platform

Tatsurou Hiraki(1), Takuma Aihara(1), Yoshiho Maeda(1), Takuro Fujii(1), Tai Tsuchizawa(1), Kiyoto Takahata(2), Takaaki Kakitsuka(2), and Shinji Matsuo(1)

(1) NTT Device Technology Labs, NTT Corporation, tatsurou.hiraki.gu@hco.ntt.co.jp

(2) Graduate School of Information, Production and Systems, Waseda University

Abstract *A 300-μm-long membrane InGaAsP electro-absorption modulator (EAM) integrated on Si-waveguide circuits exhibits a 3-dB bandwidth of 50 GHz. The EAM shows high linearity, low loss (< 4 dB), and eye openings for 112-Gbit/s PAM4 signals at wavelengths from 1570 to 1600 nm.*

Introduction

With increasing Internet traffic, low-cost, low-power-consumption, and large-capacity optical transceivers are required in datacenter networks, where directly modulated lasers (DMLs), electro-absorption modulators (EAMs), and Mach-Zehnder modulators (MZMs) are required for the appropriate modulation speed, modulation format, and transmission distance, respectively. Recently, using a III-V/Si heterogeneous integration approach, we have demonstrated low-power-consumption DMLs[1] and distributed-feedback-laser-integrated III-V MZMs[2] on a Si platform. Therefore, we also have to develop a III-V EAM with a large electro-optic (EO) bandwidth and large optical bandwidth. An InP-based EAM on a Si platform has been developed using a typical vertical *p-i-n* diode structure[3]. It showed a large extinction ratio due to the quantum confined Stark effect, and relatively low loss. However, its capacitance is much larger than that of recently developed Ge-based lateral *p-i-n* diode EAMs[4]. Therefore, whereas the Ge-based EAM provide low dynamic energy consumption and over 50-GHz bandwidth without a 50-ohm termination, an InP-based EAM on Si requires a complex traveling-wave-electrode configuration and consumes large power for high-speed operation.

As a promising solution, we focus on a membrane InP-based lateral diode, which provides low capacitance and is suitable for integration with lasers. In our previous work, by combining direct wafer bonding and epitaxial regrowth, we were able to integrate membrane InP-based lasers and MZMs with Si waveguide circuits[2]. Using this fabrication technology, in this work, we integrated a membrane InGaAsP EAM on Si waveguide circuits. In the device, the lateral electric field efficiently changes the absorption coefficient in the multiple quantum well (MQW) layer owing to exciton ionization[5] and two-dimensional (2D) Franz-Keldysh effect (FKE)[6]. A problem with the membrane device is that when the input optical power is large, generated photocarriers cause electric field screening. To solve this problem, we carefully designed a supermode between III-V and Si waveguides and fabricated an EAM with a large absorption length (300 μm). As a result, when the fiber input power was 10 dBm, we obtained 50-GHz bandwidth without 50-ohm termination thanks to the low-capacitive lateral *p-i-n* diode structure. Using the EAM, we demonstrated dynamic modulations for 112-Gbit/s 4-level pulse amplitude modulation (PAM4) signals at wavelengths from 1570 to 1600 nm.

Design

Fig. 1 shows a schematic of the InGaAsP EAM. A 600-nm-wide six-period MQW core with a photoluminescence peak of 1520 nm was buried in a 230-nm-thick InP layer. A 220-nm-thick Si-waveguide core was connected to a 3-x-3-μm^2 silica-based (SiOx) core through an inverse-taper spot-size converter (SSC) for low-loss fiber coupling. The EAM was connected to the Si core through InP inverse tapers[7].

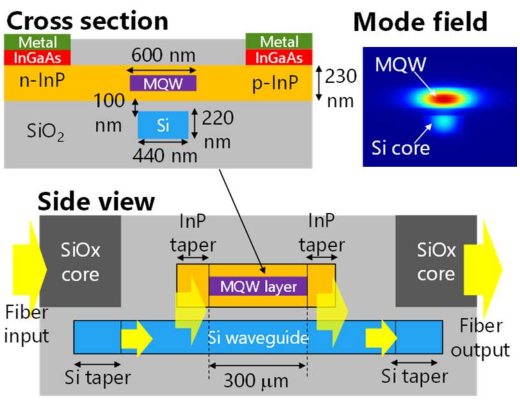

Fig. 1: Schematic of InGaAsP EAM.

By applying reverse voltage to the lumped-element electrode, a lateral electric field was almost uniformly applied to the MQW core. The

2D-FKE results in a relatively large change in the absorption coefficient near the band edge[6]. Fig. 2 shows the calculated absorption spectrum of the InGaAsP QW layer with various lateral electric fields. In the calculation, we assumed a parabolic band model, and we did not consider excitons ionized by very low reverse bias when we use the lateral diode structure. The horizontal axis is wavelength detuning from the electron-heavy-hole transition energy of a QW. When the electric field is changed from 10 to 60 kV/cm by applying external voltages, the absorption coefficient is changed from 27 to 473 cm^{-1} at the detuning of 80 nm.

To suppress electric field screening, we used a III-V/Si supermode waveguide (the calculated mode field pattern is shown in Fig. 1). Although large part of the power is confined in the 230-nm-thick III-V layer, the total fill factor into the QW layers was designed to be 9.4%, which is around one third of the fill factor of our previous phase modulator. In addition, by coupling the MQW core to the 440-nm-wide Si core, we can reduce the overlap with the *p*-InP region while maintaining a large overlap with the QW layers[7], which is important for reducing large carrier-induced loss at the *p*-InP region. Therefore, our low-loss MQW/Si core is beneficial for increasing the absorption length, which is the key to increasing the extinction ratio and supressing electric field screening at high optical input power. Despite we designed 300-μm-long absorption length, we can expect a large EO bandwidth thanks to the membrane lateral diode.

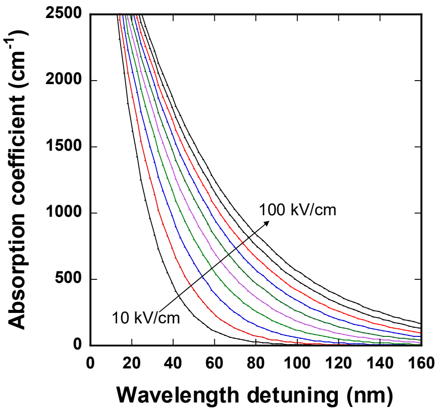

Fig. 2: Calculated absorption coefficient with lateral electric field.

Measured results

First, we measured the transmission spectrum of the fabricated EAM. Fabrication procedue was the same as our previous work[8]. Fig. 3(a) shows the normalized transmittance at various wavelengths. The vertical axis was normalized by the transmittance at 0 V. High linearity was obtained at the long wavelengths, which helps us to demonstrate PAM4 operations. Fig. 3(b) shows the measured extinction ratio at 3 V. At wavelengths from 1570 to 1600 nm, the extinction ratios range from 5.9 to 2.8 dB. Notably, the extinction ratio can be further improved by increasing the number of the QWs. Fig. 3(c) shows the measured fiber-to-fiber transmittance at 0 V along with the transmittance of a refrence Si waveguide. The on-chip loss of the EAM was less than 4 dB at the wavelength over 1570 nm. The loss decreased with increasing detuning and became almost constant. The remaining loss mainly arises not only from carrier-induced absorpiton but also from scattering and coupling losses at the InP tapers.

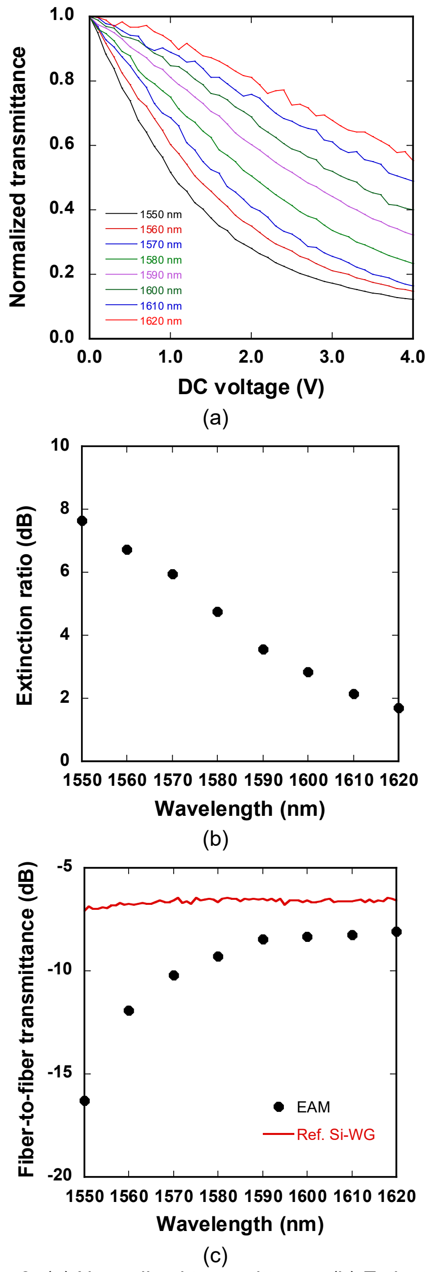

Fig. 3: (a) Normalized transmittance. (b) Extinction ratio at 3 V and (c) fiber-to-fiber transmittance at 0V.

Fig. 4(a) shows the measured frequency response of the fabricated EAM at the DC voltage, fiber input power, and wavelength of 2.0 V, 8.3 dBm, and 1570 nm, respectively. Here, we measured the device without a 50-ohm termination. Despite the 300-μm absorption length and unterminated configuration, we achieved the large EO bandwidth of around 50 GHz. The low-capacitive lateral diode structure contributes to reducing the capacitance and CR time constant. In the EAM, the input light was gradually absorbed in the entire large absorption volume, which is beneficial for reducing the maximum density of photocarriers in the QW layer and supressing electric-field screening at high input optical power. Fig. 4(b) shows the measured fiber input power dependence of the EO bandwidth with various DC voltages. With increasing DC voltage, the bandwidth becomes larger and electric-field screening is suppressed. The EO bandwidth at 2 V was over 50 GHz up to the fiber input power of 10 dBm.

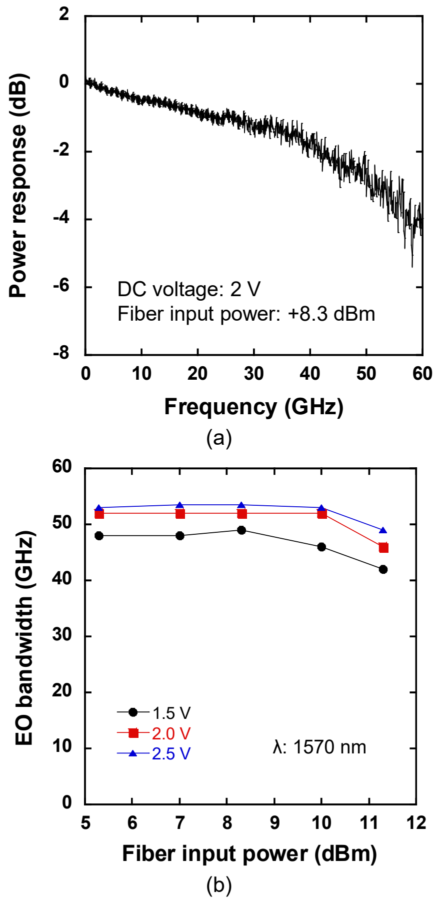

Fig. 4: (a) Frequency response at 2 V. (b) Fiber input power dependence of EO bandwidth.

Next, we input 56-Gbit/s non-return-to-zero (NRZ) signals to the EAM. The input voltage swing measured by a sampling oscilloscope was around 2 V. We applied the signals to the EAM through an RF probe without 50-ohm termination. Fig. 5(a) shows the measured eye diagram at the DC bias and wavelength of 2 V and 1590 nm, respectively. The eye clearly opened with the extinction ratio of 5.6 dB due to the large EO bandwidth. We also input 112-Gbit/s PAM4 signals to the EAM. The input waveform is shown in Fig. 5(b). Fig. 5(c)-(f) show the measured eye diagrams at wavelengths from 1570 to 1600 nm. In the experimental setup, we used a *p-i-n* photodetector directly connected to the sampling oscilloscope. The eye opened with relatively good linearity in the 30-nm optical bandwidth. In this work, the wavelength range was limited by the optical bandwidth of the erbium-doped amplifier in our experimental setup.

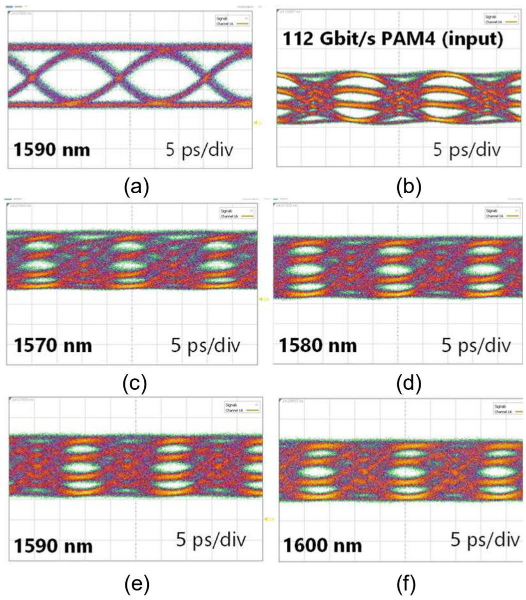

Fig. 5: (a) Measured eye diagram for 56-Gbit/s NRZ signals. (b) Input signal for 112-Gbit/s PAM4. Output waveforms at wavelengths of (c) 1570, (d) 1580, (e) 1590 and (f) 1600 nm.

Conclusion

We demonstrated 112-Gbit/s PAM4 operation in the optical bandwidth of 30 nm using a membrane InGaAsP EAM on a Si platform. This technology is key to fabricating low-cost, large-capacity, and low-power-consumption optical transceivers.

References

[1] S. Matsuo *et al.*, "Directly modulated buried heterostructure DFB laser on SiO_2/Si substrate fabricated by regrowth of InP using bonded active layer", *Opt. Express.*, vol. 22, issue 10, pp. 12139-12147, 2014.

[2] T. Hiraki *et al.*, "Integrated DFB Laser Diode and High-efficiency Mach-Zehnder Modulator using Membrane

III-V Semiconductors on Si Photonics Platform", in *IEEE IEDM Tech. Deg.,* San Francisco, United States, Dec. 2019, 33.4.

[3] Y. Tang *et al.*, "Over 67 GHz bandwidth hybrid silicon electroabsorption modulator with asymmetric segmented electrode for 1.3 µm transmission", *Opt. Express,* vol. 20, no. 10, pp. 11529-11535, 2012.

[4] S. A. Srinivasan *et al.*, "56 Gb/s germanium waveguide electro-absorption modulator", *IEEE J. Lightw. Technol.,* vol. 34, no. 2, pp. 419-424, 2016.

[5] D.A.B. Miller *et al.*, "Electric field dependence of optical absorption near the band gap of quantum-well structures," *Phys. Rev. B.*, vol. 32, no. 2, pp. 1043-1060, 1985.

[6] F.L. Lederman *et al.*, "Theory of electroabsorption by anisotropic and layered semiconductors. I. Two-dimensional excitons in a uniform electric field", *Phys. Rev. B.,* vol. 13, no. 4, pp. 1633-1642, 1976.

[7] T. Hiraki *et al.*, "Membrane InGaAsP Mach–Zehnder Modulator Integrated With Optical Amplifier on Si Platform", *IEEE J. Lightw. Technol.,* vol. 38, no. 11, pp. 3030-2036, 2020.

[8] T. Aihara *et al.*, "Membrane III-V/Si DFB Laser Using Uniform Grating and Width-Modulated Si Waveguide", *IEEE J. Lightw. Technol.,* vol. 38, no. 11, pp. 2961-2967, 2020.